View metadata, citation and similar papers at core.ac.uk

brought to you by CORE

provided by Flinders Academic Commons

Flinders UNIVERSITY

Archived at the Flinders Academic Commons:
http://dspace.flinders.edu.au/dspace/

This is a copy of an article published in *Infection and Immunity,* and is available online at:
http://iai.asm.org/content/81/7/2574.full?sid=fd90da76-0ac3-46b8-b644-a3471d9c7c45

Please cite this as: Eijkelkamp, B.A., Stroeher, U.H., Hassan, K.A., Elbourne, L.D.H., Paulsen, I.T. and Brown, M.H., 2013. H-NS plays a role in expression of Acinetobacter baumannii virulence features. Infection and Immunity, 81(7), 2574-2583.

DOI: http://dx.doi.org/10.1128/IAI.00065-13

© 2013 American Society for Microbiology. Paper reproduced here with permission from the publisher.

1 H-NS Plays a Role in Expression of *Acinetobacter baumannii* Virulence Features

2 Running title: The *A. baumannii* H-NS protein

3 Bart A. Eijkelkamp[a], Uwe H. Stroeher[a], Karl A. Hassan[b], Liam D.H. Elbourne[b], Ian T. Paulsen[b]
4 and Melissa H. Brown[a#]

5 [a] School of Biological Sciences, Flinders University, Adelaide, South Australia, Australia

6 [b] Department of Chemistry and Biomolecular Sciences, Macquarie University, Sydney, New
7 South Wales, Australia

8 [#] melissa.brown@flinders.edu.au

9 Current address

10 Bart A. Eijkelkamp

11 School of Molecular and Biomedical Science

12 University of Adelaide

13 Adelaide, SA 5005, Australia

14

ABSTRACT

Acinetobacter baumannii has become a major problem in the clinical setting with the prevalence of infections caused by multi-drug resistant strains on the increase. Nevertheless, only a limited number of molecular mechanisms involved in the success of *A. baumannii* as a human pathogen have been described. In this study, we examined the virulence features of a hyper-motile derivative of *A. baumannii* strain ATCC 17978, which was found to display enhanced adherence to human pneumocytes and elevated levels of lethality towards *Caenorhabditis elegans* nematodes. Analysis of cellular lipids revealed modifications to the fatty acid composition, providing a possible explanation for the observed changes in hydrophobicity and subsequent alteration in adherence and motility. Comparison of the genome sequences of the hyper-motile variant and parental strain revealed that an insertion sequence had disrupted a *hns*-like gene in the variant. This gene encodes a homologue of the histone-like nucleoid structuring (H-NS) protein, a known global transcriptional repressor. Transcriptome analysis identified the global effects of this mutation on gene expression, with major changes seen in the autotransporter Ata, a type VI secretion system and a type I pili cluster. Interestingly, isolation and analysis of a second independent hyper-motile ATCC 17978 variant revealed a mutation to a residue within the DNA binding region of H-NS. Taken together, these mutants indicate that the phenotypic and transcriptomic differences seen are due to loss of regulatory control effected by H-NS.

INTRODUCTION

Acinetobacter baumannii is widely recognized as a highly multi-drug resistant pathogen that causes major problems in hospitals globally (1, 2). Antimicrobial resistance in *A. baumannii* has been extensively studied and resistance determinants novel to *Acinetobacter* are being identified regularly. These resistance genes can often be found on horizontally-acquired genetic material, increasing the risk of generating pan-resistant clones. As such, global dissemination of these multi-drug resistant clones poses a serious threat. Furthermore, biofilm formation has also previously been associated with increased resistance and survival as well as immune evasion and may therefore play a significant role in *A. baumannii* pathogenicity. Adherence characteristics, such as biofilm formation and binding to eukaryotic cells, have been studied in a large number of *A. baumannii* strains (3-9) and are but one of many potential factors involved in virulence. An additional factor that can influence virulence potential is motility; two distinct forms of surface migration have been described for this species (3, 7, 10-12). Expression of these phenotypes varies between strains and to a degree clonal groups, such as the conserved expression of twitching motility by isolates in the international clone I group (3). Although motility has been associated with increased biofilm formation and virulence in other bacteria, such as *Pseudomonas aeruginosa* and *Dichelobacter nodosus* (13-18), the significance of motility in the virulence potential of *A. baumannii* remains to be confirmed.

Various molecular mechanisms contributing to the virulence potential of *A. baumannii* have been identified (19). For example, one of the most extensively studied virulence determinants in *A. baumannii* is OmpA, which not only facilitates adherence to eukaryotic cells and abiotic surfaces but also mediates invasion and promotes cell death of lung epithelial cells (20-24). The penicillin

binding protein-7/8, phospholipase D, lipopolysaccharides and production of K1 capsule in *A. baumannii* have also been shown to play important roles in survival in a host environment (25-28). Furthermore, phospholipase D facilitates bacterial crossing of the blood-lung barrier, as shown in a rat model system (26). More recently, siderophore mediated iron-acquisition mechanisms have been demonstrated to be essential for lethality in mice (29). Many virulence determinants described in other Gram-negative pathogens have been identified in the genome sequences of *A. baumannii*, such as the type VI secretion system (30, 31). However, to date, their role in virulence and persistence of *A. baumannii* has not been characterized.

The regulatory networks controlling expression of *A. baumannii* virulence determinants, such as iron acquisition, motility, attachment and biofilm formation, remain largely unknown. Transcriptomic studies have indicated that the ferric uptake regulator (FUR) is the primary regulator of *A. baumannii* iron-acquisition mechanisms (10, 32) and a number of studies have shown that quorum-sensing influences both motility and biofilm formation (12, 33, 34). Additionally, a two-component regulatory system, encoded by *bfmRS*, plays a critical role in the regulation of the Csu type I pili, which may influence attachment and motility (35).

It is likely that *A. baumannii* has also acquired virulence factor genes via exogenous DNA uptake. In other bacterial genera, transcriptional regulation of horizontally-acquired genetic material is in part controlled by the histone-like nucleoid structuring (H-NS) protein and provides a level of protection against expression of genes that encode products with detrimental effects to the host bacteria (36, 37). Although *Acinetobacter* spp. are known to possess large quantities of horizontally-acquired genetic material, to date, the function of H-NS in *A. baumannii* has not been described.

This study describes the comprehensive characterization of a hyper-motile derivative of *A. baumannii* strain ATCC 17978. Whole genome sequencing of this strain revealed the insertional inactivation of a gene encoding the global regulator H-NS. Beyond the dramatic changes observed with respect to motility, the mutant strain also displayed altered adherence phenotypes to biotic surfaces, as well as an increase in virulence using a *Caenorhabditis elegans* model system. In summary, this study describes the importance of H-NS in expression of *A. baumannii* persistence and virulence genes.

MATERIALS AND METHODS

Bacterial strains

Acinetobacter strain ATCC 17978 (CP000521) was obtained from the American Type Culture Collection (ATCC) and *E. coli* OP50 was kindly provided by Hannah Nicholas (The University of Sydney). Freeze-dried *Acinetobacter* cells were revived as recommended by the ATCC and colony material from the overnight cultures grown on Luria-Bertani (LB) media were transferred to a cryopreservation tube containing 20% glycerol in LB broth and placed at -80°C for long term storage. The isolated variants, i.e. 17978hm and HNSmut88 were similarly stored. For subsequent culturing purposes, material was scraped from the top of the frozen stocks and streaked onto LB media.

Biofilm assays

The static biofilm formation assay was performed as described previously (3). In brief, overnight cultures were diluted 1:100 in fresh Mueller-Hinton (MH) broth in polystyrene microtiter trays and incubated overnight at 37°C. Adherent cells were washed once with phosphate buffers saline

(PBS), stained by incubation with 0.1% crystal violet for 30 minutes at 4°C, and washed three times with PBS. Dye was released from the cells using ethanol:acetone (4:1) and shaking at 200 rpm for 30 minutes at room temperature. Absorbance was measured at 595 nm on a Fluostar Omega spectrometer (BMG Labtech, Offenburg, Germany).

Pellicle formation assays

Pellicle formation assays were based on a method used previously (6). Overnight bacterial cultures in LB broth were diluted in fresh LB broth containing 100 mM NaCl. Pellicle formation assays were performed in polypropylene tubes and were incubated at room temperature without shaking for 72 hours. The pellicle film was separated from the tube by the addition of methanol. The pellicle biomass was measured (OD_{600}) after resuspending pelleted cells in 1 ml PBS. The experiments were performed at least three times.

Eukaryotic cell adherence assays

The adherence of *A. baumannii* cells to A549 human pneumocytes was investigated as described previously (3). Cell lines were grown in Dulbecco's Modified Eagle medium (Invitrogen, Australia) supplemented with 10% fetal bovine serum (Bovogen, Australia). Prior to use, the cell monolayer was examined microscopically to ensure >95% coverage. Washed A549 monolayers in 24-well tissue culture plates were subsequently infected with a bacterial inoculum containing ~$1x10^7$ colony forming units (CFU). After incubation at 37°C for 4 hours, culture medium was removed, and the monolayers washed three times with 1 ml of PBS. Cell monolayers were detached from the plate by treatment with 100 µl of 0.25% trypsin and 0.02% EDTA in PBS. Eukaryotic cells were subsequently lysed by the addition of 400 µl 0.025% Triton X-100 and serial 10-fold dilutions thereof were plated on LB agar to determine the number of CFU of

adherent bacteria per well. Collated data for adherence assays were obtained from at least three independent experiments and represent the data points for each experiment of quadruplicate wells. The CFU of the cell culture medium after 4 hours incubation was determined to ensure that strains did not display differences in their respective growth rates during the adherence assay.

Caenorhabditis elegans *killing assays*

C. elegans N2 nematodes were synchronized in their development by initially placing nematode eggs onto *E. coli* OP50 seeded nematode growth media (NGM) (38). The larval L3/L4 stage nematodes were harvested and placed on NGM agar plates seeded with *A. baumannii* strains. Viability of at least 200 individual nematodes found in random fields of view were determined by microscopic examination. The viability was determined at 24 hours intervals for up to 144 hours and expressed as a percentage of live nematodes. The results (n=4) represent duplicate experiments performed on two different days. Two independent researchers determined the viability of the nematodes in a 'blind' experiment.

Cell surface hydrophobicity tests

Cell surface hydrophobicity was examined as described previously (39). The OD of the cell suspensions before ($OD_{initial}$) and after addition of xylene (OD_{final}) was measured at 600 nm. Experiments were performed three times. The hydrophobicity index (HI), expressed in percentage, was calculated using the following formula; HI (%) = (OD_{intial} - $OD_{final}/OD_{initial}$)*100. Experiments were performed at least three times.

Phenotype MicroArray analysis

A. baumannii ATCC 17978 WT and 17978hm mutant strains were cultured on LB agar overnight. Cells were transferred to 1x IF-0 inoculation fluid (BIOLOG, Inc.) to 42% transmittance. Cells were then diluted 1:5 in 1x IF-0 containing dye A (BIOLOG, Inc.) with a final transmittance of 85%. 100 µl of the cell suspensions were transferred to each well of Biolog MicroPlate™ PM01 and PM02A plates. Plates were incubated in the OmniLog® Phenotype MicroArray System (Biolog, Inc.) at 37°C for 48 hours, with readings taken every 15 minutes. Data from the WT and mutant strains were overlaid using the OmniLog® File Management/Kinetic Analysis software v1.20.02 and analyzed using OmniLog® Parametric Analysis software v1.20.02 (Biolog, Inc.).

Fatty acid analyses

The strains for fatty acid analysis were grown for 8 hours on MH plates containing 0.25% agar. Cells were collected and washed with pre-chilled PBS. Total cellular lipids were extracted using chloroform/isopropanol and were subsequently methylated using a 1% sulphuric acid solution in methanol, as described previously (40). The fatty acid methyl esters were separated by gas chromatography at the School of Agriculture, Food and Wine, University of Adelaide. The abundance of each fatty acid was expressed as the percentage of the total of all fatty acids. All analyzed bacterial strains were prepared on two separate occasions and the data represent the average over those two experiments.

RNA isolation

Cells used for measurement of transcription levels were harvested from semi-solid MH media (0.25% agar) using pre-chilled PBS. The cells were subsequently pelleted by centrifugation and

lysed in TRIzol® reagent (Invitrogen, Australia) and chloroform. Following phase separation by centrifugation, RNA was extracted from the aqueous phase using a RNA isolation kit (Bioline). DNaseI (Promega) treatment was performed as per the manufacturer's recommendations.

Transcriptome analysis

We used a custom genomic microarray for *A. baumannii* ATCC 17978, as previously described (10). The results represent data obtained from three biological replicates and a dye-swap experiment. The array was designed to harbor at least four probes per gene. The transcriptomic data have been deposited into the gene expression omnibus database (http://www.ncbi.nlm.nih.gov/geo/) and can be accessed using the accession number GSE40681.

Quantitive Reverse Transcription PCR

cDNA was synthesized using random hexamers (GeneWorks, Australia) and M-MLV reverse-transcriptase (Promega) as per the manufacturer's recommendations. Oligonucleotides used in this study were designed using Primer3 (41) as an integral part of UGENE v1.6.1 (Unipro) and are listed in Table S1. qPCR was performed on a Rotor-Gene RG-3000 (Corbett Life Science, Australia) using DyNAmo SYBR® green qPCR kits (Finnzymes, Australia). Internal qPCR controls used primers designed to 16s rRNA (A1S_r01) to ensure differences seen are due solely to alterations in the target gene expression and not due to mRNA quality or quantity. Transcriptional differences were calculated using the $\Delta\Delta C_t$ method (42) and the data represent experiments performed in biological triplicates.

Genome sequence analysis

A. baumannii ATCC 17978 and 17978hm were sequenced using Illumina BeadArray technology, performed by the Ramaciotti Centre for Gene Function Analysis, University of New South Wales, Australia. The whole genome shotgun sequence reads were assembled using Velvet 1.1 (43).

Genetic complementation of the hyper-motile A. baumannii mutant strains

The *hns* PCR product was cloned into *Bam*HI digested pWH1266 (44). Electro-competent *A. baumannii* cells freshly prepared on the day of use were incubated on ice with plasmid DNA for 5 minutes followed by electroporation using a MicroPulser (Bio-Rad) at 2.5 kV, 200Ω and 25 µF. After recovery in 1 ml of LB media for at least 1 hour at 37°C, cells were cultured overnight at 37°C on LB media containing 200 µg/ml ampicillin.

RESULTS AND DISCUSSION

Isolation of hyper-motile variant strains

Contrary to their original designation as non-motile, a number of *A. baumannii* strains have been shown to participate in various forms of motility when grown under appropriate conditions (3). Motility of strain *A. baumannii* ATCC 17978 is evident on semi-solid Luria-Bertani (LB) media containing <0.5% agar (3, 10, 12), with concentrations of agar above this level inhibiting the phenotype. However, we observed two distinct morphologies in a cryopreserved ATCC 17978 stock cultured on LB medium containing 1% agar. The colony morphology of one variant appeared non-motile as per wild-type (WT) ATCC 17978, whereas the other displayed a motile appearance, which was designated as a hyper-motile phenotype. To examine the motility of these

variants, five individual hyper-motile colonies were inoculated in the center of both LB and Mueller-Hinton (MH) media containing different concentrations of agar. The phenotype was most distinct using MH containing 0.25% agar, conditions non-permissive for motility of WT cells. Whereas four out of five hyper-motile variants were equally motile and covered the entire surface of the plate within eight hours (migration ~45 mm), one hyper-motile variant was found to be delayed by approximately two hours compared to the other hyper-motile variants. This indicated that at least two distinct variants of the parental strain were isolated. To examine potential genotypic differences that may explain the altered phenotypic characteristics, one of the hyper-motile strains displaying motility on semi-solid MH media, designated 17978hm, and the parent WT ATCC 17978 strain were selected for further analyses.

Sequence analysis of the hyper-motile A. baumannii ATCC 17978 derivatives

The genetic differences between the *A. baumannii* strain 17978hm and ATCC 17978 were assessed by sequencing both their genomes using Illumina BeadArray technology. Sequence reads were assembled using Velvet 1.1 (43), generating 245 contigs for strain 17978hm and 292 contigs for strain ATCC 17978. Whole genome alignments were generated using Mauve, and the ATCC 17978 genome sequence reported by Smith *et al*., 2007 (CP000521) was included for comparative purposes.

The most striking finding from comparative analyses of the parental and 17978hm genome sequences was an insertion sequence (IS) element found in the *hns* (A1S_0268) locus of strain 17978hm (Fig. 1A). In other bacteria, H-NS has been shown to act as a global repressor that preferentially binds AT-rich DNA sequences (36, 37). Spontaneous insertional inactivation of *hns*, as observed in strain 17978hm, has also been described in *Mycobacterium smegmatis* (45).

Interestingly, the *M. smegmatis* H-NS mutant strain was also found to display a hyper-motile phenotype (39). The H-NS protein is well conserved between *Acinetobacter* strains; the ATCC 17978 H-NS protein sequence is 100% identical to that from strains AYE and SDF, and 92% identical to H-NS from *Acinetobacter baylyi* ADP1. The ATCC 17978 genome only encodes a single copy of *hns* and to date, strain AB058 is the only *A. baumannii* strain found to harbor two *hns*-like genes (data not shown).

Analysis of the DNA sequence revealed that transposition of an IS element into *hns* in strain 17978hm had occurred with nine nucleotides of the *hns* target sequence being duplicated and now flanking the termini of the IS element (Fig. 1A). The sequence of this IS element exhibited >99% identity to an IS element harboring A1S_0628 which encodes a putative transposase in strain ATCC 17978, raising the possibility that the IS element identified within the *hns* locus of strain 17978hm was generated by a transposition event. Two similar transposases found in strain 17978hm and ATCC 17978, designated A1S_2554 and A1S_1172, showed 97% and 84% sequence identity to A1S_0628, respectively, and as such are unlikely to be the originator of the insertion.

As mentioned above, a total of five hyper-motile variants were isolated in this study. The *hns* gene of the four other hyper-motile strains was PCR amplified and sequenced. Three of these were found to possess an insertion disruption identical to that seen in strain 17978hm and also displayed a hyper-motile phenotype similar to 17978hm (data not shown). The *hns* gene of the variant displaying a less pronounced level of hyper-motility (motility delayed by two hours on semi-solid MH media compared to strain 17978hm) contained a single nucleotide polymorphism, resulting in a lysine to isoleucine substitution at position 88 of the H-NS protein ($H\text{-}NS_{K88I}$). Interestingly, lysine 88 is part of the DNA-binding domain of H-NS-like proteins (46) (Fig. 1B).

Lacking this positively-charged residue may have resulted in an altered affinity for regulatory binding sites and consequently reduced repression of the genes encoded downstream. As mentioned, the *A. baumannii* strain expressing the H-NS$_{K88I}$ protein, designated HNSmut88, displayed an intermediate hyper-motile phenotype compared to strain 17978hm, which was investigated by comparing the positively charged residues in the DNA binding domain to those in other H-NS-like proteins, such as Lsr2 from *Mycobacterium tuberculosis*, H-NS from *Salmonella* and Ler from *Escherichia coli* (46, 47). Whereas the *Salmonella* H-NS and *E. coli* Ler proteins contain a single positively charged residue in the DNA binding domain, the *M. tuberculosis* Lsr2 and *A. baumannii* H-NS contain two; in *A. baumannii* H-NS these are lysine and arginine at position 88 and 86, respectively (Fig. 1B). Previous mutagenesis studies in *M. tuberculosis* have shown a significant level of Lsr2 DNA binding in mutants where only a single positive charged residues in the DNA binding domain was removed (47). However, double mutants in Lsr2, or mutation of the single charged residue present in the DNA binding domain of the *Salmonella* H-NS resulted in a complete lack of binding (47). Therefore, arginine 86 may be sufficient to maintain significant binding affinity of H-NS$_{K88I}$ to certain regulatory targets explaining the intermediate motility phenotype observed in this strain. Although the *A. baumannii* H-NS and *E. coli* Ler proteins possess an arginine adjacent to the DNA-binding domain (Fig. 1B), when present as the sole positively charged residue in this region of the protein it does appear to be insufficient for maintaining the ability to bind its targets (46).

To confirm that the altered phenotypes observed in the hyper-motile *A. baumannii* variants were a result of mutations in *hns*, the WT *hns* gene was cloned into the *E. coli-Acinetobacter* shuttle vector pWH1266, producing pWH0268, and used for complementation in the mutant strains. Motility assays revealed that introduction of pWH0268 into *A. baumannii* strains 17978hm and

HNSmut88 resulted in loss of the hyper-motile phenotype on solid LB media and semi-solid MH media, returning the phenotype to that observed for WT cells (data not shown). Due to the reduced severity of phenotypic changes observed in HNSmut88 compared to 17978hm, only the ATCC 17978 and 17978hm strains were assessed in subsequent phenotypic and transcriptional analyses.

Adherence characteristics

Biofilm formation is a complex process initiated by attachment to a surface, followed by the formation of a multilayered biomass containing secondary structures. It was hypothesized that the adherence characteristics of strain 17978hm may differ to that of WT cells since changes in motility could affect biofilm formation, as previously reported for *P. aeruginosa* (18). However, adherence to the surface of a polystyrene microtiter tray showed no major differences between the WT and hyper-motile strains (data not shown). In contrast, pellicle formation, i.e., the biofilm at the air-liquid interface, appeared significantly higher in 17978hm as compared to the WT strain or its complemented derivative 17978hm (pWH0268) (Fig. 2A). The level of pellicle biomass in strain 17978hm (pWH0268) was higher than that observed for the WT strain, which could be a result of loss of the complementation plasmid over the 72 hours incubation period. Pellicle formation was only observed in LB media at 25°C and not at 37°C (data not shown), which corroborates data from similar studies on *Acinetobacter* spp. (6). Attempts to demonstrate pellicle formation by strains grown in MH media was unsuccessful. During static culturing for pellicle formation, it was apparent that the planktonic growth of the pellicle forming 17978hm cells was lower than that of the non-pellicle forming WT cells, OD_{600} = ~0.15 and ~0.50, respectively. The differences in planktonic growth may be due to a reduction of oxygen levels in

293 the growth medium of strain 17978hm as a result of the high oxygen dependency of the pellicle,
294 a phenomenon described previously (48).

295 Adherence to abiotic and biotic surfaces appears to be mediated by different molecular
296 mechanisms in most *A. baumannii* strains and as such does not always correlate (3, 5, 49).
297 Therefore, despite similar abiotic adherence levels observed in microtiter trays, adherence to
298 biotic surfaces by strains ATCC 17978, 17978hm, 17978hm (pWH1266) and 17978hm
299 (pWH0268) was investigated. A549 pneumocytes were selected for these experiments to mimic
300 adherence to the epithelial layer of the human lung (50). After incubating the bacteria in
301 conjunction with pneumocytes for 4 hours, the number of 17978hm cells adhered to and
302 potentially intracellularly located in the washed A549 eukaryotic cells was enumerated and
303 found to be significantly higher than the number of ATCC 17978 cells (~1.6-fold; $p<0.05$) (Fig.
304 2B). Interestingly, adherence levels of 17978hm (pWH0268) cells were lower than those for WT
305 cells, indicating a possible dose-dependent effect due to a difference in plasmid copy number
306 (35), where H-NS may be more abundant in the complemented cells. The increased adherence
307 potential of strain 17978hm to human pneumocytes may indicate that 17978hm cells have higher
308 persistence levels during infection and more specifically, pneumonia. Further work using a
309 mouse pneumonia model may reveal whether the differences seen in adherence to pneumocytes
310 play a biological significant role in the disease process.

311 *The hyper-motile variant possesses an increased virulence potential*

312 Since 17978hm showed a significantly increased ability to adhere to eukaryotic cells its disease
313 potential was investigated further, by examining ATCC 17978 and 17978hm strains for their
314 ability to kill *C. elegans* nematodes. Measureable death of the *C. elegans* nematodes was

observed between 72 and 144 hours incubation on either WT or 17978hm cells (Fig. 3). A significant difference between the percentage of live nematodes incubated with either WT or 17978hm cells was observed at 120 hours and 144 hours (Fig. 3). At both time points, approximately 20% higher death rates were observed for nematodes incubated with 17978hm cells compared to those with WT cells (Fig. 3). The experiment was terminated after 144 hours as the remaining live nematodes were consuming the disintegrated dead nematodes at time points beyond 144 hours, making it difficult to accurately determine the percentage of live versus dead nematodes during the latter part of the experiment (data not shown).

Cell surface hydrophobicity and fatty acid composition

The differences between the phenotypes of the WT and hyper-motile *A. baumannii* cells described above may be related to changes at the cell surface. Therefore, the hydrophobicity of WT and 17978hm cells was investigated using the microbial adhesion to hydrocarbons (MATH) test (39); an increase in the hydrophobicity index (HI) of 17978hm cells (HI = 65%) compared to WT cells (HI = 44%) was observed (Table 1). When a WT copy of *hns* (carried on pWH0268) was introduced into 17978hm cells, the hydrophobicity decreased significantly, returning to levels lower than those observed for ATCC 17978 cells.

To investigate a potential cause for the change in cell surface hydrophobicity, the total fatty acid compositions of WT and 17978hm cells, and 17978hm (pWH1266) and 17978hm (pWH0268) were determined. In a study on *Listeria innocua*, decreases in the ratio between C_{15} and C_{17} saturated fatty acids were linked to increases in cell surface hydrophobicity (51). Similarly, in this study the percentage of C_{17} fatty acid was significantly higher in the hyper-motile strains,

which may explain the differences observed in cell surface hydrophobicity (Table 1). Major changes in the concentrations of other fatty acids were not observed.

Transcriptomic analysis of the motile versus non-motile population

Comparative analysis of the transcriptomes of cells in distinct life styles may provide information about the molecular mechanisms and regulatory pathways responsible for driving a population into a certain mode of living. Therefore, we employed a whole genome microarray to examine the effect of the *hns* inactivation on the transcriptome of *A. baumannii*. Major differences were observed between the transcriptomes of the hyper-motile 17978hm and non-motile WT cells (Fig. 4). More than 4-fold differential expression was seen for 152 genes, of which 91 were down- and 61 up-regulated (Table S2; GEO:GSE40681). The most striking differences were observed in the quorum-sensing regulated genes homoserine lactone synthase (A1S_0109) and the homoserine lactone responsive regulator (A1S_0111), which were both heavily up-regulated. Furthermore, an adjacent cluster involved in the production of secondary metabolites, putatively lipopeptides or polyketides, was up-regulated by more than 100-fold. Both quorum-sensing and the adjacent cluster have been shown to play an important role in motility of *A. baumannii* (12).

Various genes encoding surface-presented structures were also heavily up-regulated in *A. baumannii* strain 17978hm. The autotransporter Ata (A1S_1032) was overexpressed by approximately 10-fold. In a recent report, Ata was found to play a major role in adherence and virulence of *A. baumannii* strain ATCC 17978 (52), potentially explaining the increased virulence levels of strain 17978hm observed in the *C. elegans* killing assays described above. This gene appears to be transcriptionally linked to A1S_1033 (8-fold up-regulation), the product

of which shares homology with putative OmpA-like proteins (20-24). Even though there is no evidence of a role for type I pili in promotion of surface translocation in *A. baumannii*, four genes encoding a novel type I pili cluster (A1S_1507-1510) were up-regulated by more than 10-fold. Other phenotypes, such as increased adherence to human epithelial cells or increased pellicle formation, may be associated with overexpression of type I pili in the hyper-motile strain. A gene cluster predicted to encode a type VI secretion system (A1S_1292-1311) was found to be up-regulated in the motile population. Type VI secretion systems can contribute to bacterial pathogenicity as observed in *P. aeruginosa* (53), however, the role of these systems in *A. baumannii* is yet to be elucidated (54). It would appear not to be essential for full virulence in a number of isolates, as comparative genomic analyses revealed that four open reading frames encoding proteins of unknown function have replaced the type VI secretion system gene cluster in *A. baumannii* strain D1279779 (AERZ00000000). The type VI secretion system may also be non-functional in strain 1656-2 (CP001921) (55), as it contains an insertion element in the gene homologous to A1S_1302. Furthermore, the gene cluster coding for the type VI secretion system can also be found in the non-pathogenic *A. baumannii* strain SDF (CU468230). Therefore, the function of the type VI secretion system in *A. baumannii* requires further investigation.

Interestingly, genes functioning in fatty acid biosynthesis, including *fabG* (A1S_0524) and *fabF* (A1S_0525), were found to be overexpressed by more than 2-fold in strain 17978hm. FabF is responsible for fatty acid elongation, which occurs in steps of two carbon additions i.e., C_{13} to C_{15} to C_{17} (56). Thus, these increases in transcription levels may be related to the increase of the C_{17} observed in 17978hm cells as compared to WT cells (Table 1).

Numerous genes functioning in metabolism were found to be down-regulated in the motile population, such as those encoding members of the phenylacetic acid degradation pathway (Fig.

4). Down-regulation of metabolic pathways was also observed in a transcriptional investigation of swarming *P. aeruginosa* cells (57). A Phenotype MicroArray™ (BIOLOG, Inc.) analysis using MicroPlates™ PM01 and PM02A was performed to obtain a comprehensive depiction of carbon-source utilization by the *Acinetobacter* strains 17978hm and ATCC 17978. The most pronounced dissimilarities between these strains were observed in the presence of L-threonine or D-malic acid, in which WT ATCC 17978 cells showed more active respiration than 17978hm cells (Table S3). The up-regulation of a putative threonine efflux transporter (A1S_3397) in 17978hm may be associated with a reduction in available threonine and consequently lower respiratory levels seen in this strain. Changes in transcription levels of genes encoding proteins involved in D-malic acid metabolism were not observed (data not shown).

Identification of potential H-NS targets in the ATCC 17978 genome

Although not previously examined in *A. baumannii*, H-NS is a well-studied protein in many bacterial genera (58, 59). Sequence homology between H-NS proteins from different bacteria is often low (<30%), however, the targets appear to be similar. Horizontally-acquired genetic material is often AT-rich and is therefore a likely target for H-NS proteins (59). Hence, the H-NS proteins are also known as xenogeneic silencers. A common example of a horizontally-acquired genomic region targeted by H-NS encodes the type VI secretion system (60). Indeed, this cluster (A1S_1292-1312) was found to be heavily up-regulated in strain 17978hm (Fig. 4). Based on the potential for H-NS to act as a xenogeneic silencer, other potential regulatory targets were identified encoded within novel genomic regions. Transcriptomic data were overlayed with the results of BLASTP comparisons of CP000521 (ATCC 17978) with six other *Acinetobacter* genomes; *A. baumannii* AB0057, ACICU, AYE, AB307-0294 and SDF, and *A. baylyi* ADP1 on a circular representation of the ATCC 17978 genome (Fig. 5). A correlation was seen between

up-regulation and lack of conservation of the respective genes/gene clusters. These non-conserved up-regulated loci were subsequently analyzed using a whole genome alignment generated in MAUVE (61) containing the genomes described above. Thirteen potential horizontally-acquired H-NS targets (Fig. 5) were identified, which included a surface protein (A1S_0745) and the autotransporter adhesin (A1S_1032) described above. Interestingly, in *E. coli*, transcription of a gene encoding the autotransporter protein UpaC was recently found to be repressed by H-NS (62), consistent with our findings. These surface presented proteins, potentially regulated by H-NS, may play a role in the phenotypic alterations of strain 17978hm. The S-adenosyl-L-methionine-dependent methyltransferase (A1S_2744), also potentially regulated by H-NS, is involved in methylation of proteins, lipids, DNA and RNA, and therefore, in controlling a wide range of cellular processes (63). The putative threonine efflux transporter protein described above (A1S_3397), also appeared to be under regulatory control of H-NS (Fig. 5). Overall, these analyses suggested that various horizontally-acquired genome regions are targets for transcriptional repression by H-NS in *A. baumannii* and inactivation of H-NS results in up-regulation of the genes within these regions.

Although H-NS is known to bind high AT-percentage regions, the global GC-skew analysis shown in the circular genome figure did not reveal such an association with transcriptional up-regulation (Fig. 5). This may be due to the generally low GC-percentage of the *A. baumannii* ATCC 17978 genome (~39%). However, when examining the upstream regions of heavily overexpressed genes, a correlation between high AT-content and transcriptional up-regulation in strain 17978hm was observed. The GC-percentage of various potential H-NS targets was as low as 20% (Fig. 6), which is significantly lower than the average GC-percentage of the ATCC 17978 genome-wide intergenic regions (~35%).

The genomic region harboring the gene encoding homoserine lactone synthase (A1S_0109) and the cluster involved in biosynthesis of polyketides/lipopeptides (A1S_0112-0119) possessed two regulatory sites with a low GC-percentage (Fig. 6). In particular, the upstream region of the biosynthesis cluster (GC content of 20%) may be targeted by H-NS. Previously, Clemmer *et al.* showed that the A1S_0112-0119 cluster is under control of quorum-sensing signals in the form of acyl-homoserine lactones via AbaR (12).

Other overexpressed genes with a putative H-NS binding region upstream included the above described autotransporter Ata and putative *ompA*-like gene (A1S_1032-1033), the type VI secretion system (A1S_1292-1312), a novel type I pili cluster (A1S_1510-1507), a cluster involved in lipoate synthesis and acetoin metabolism (A1S_1698-1704), and a small putatively secreted protein (A1S_3273) (Fig. 6).

Alanine racemases are ubiquitous in prokaryotes and are responsible for racemization of L- and D-alanine. Like most other prokaryotes, *A. baumannii* strains possess two alanine racemases, DadX (A1S_0096) mediating conversion of D- to L-alanine and Alr (A1S_2176), which facilitates L- to D-alanine racemization. However, *A. baumannii* ATCC 17978 also contains a second Alr-like alanine racemase encoded by A1S_1357. This heavily up-regulated gene in strain 17978hm (>70-fold) appeared to have been horizontally-acquired and also possessed an AT-rich upstream region making it a likely target for transcriptional repression by H-NS (Fig. 5 and 6).

Transcriptional analysis of putative H-NS regulated genes

We investigated the transcription levels of nine differentially expressed genes in the complemented strain pair, 17978hm (pWH1266) and 17978hm (pWH0268). These genes are

potential targets of H-NS based on previously described findings or the bioinformatic analysis performed in this study. Seven of these genes were highly up-regulated (>4-fold); A1S_0111, A1S_0112, A1S_1032, A1S_1292, A1S_1510, A1S_1699 and A1S_3273, and two highly down-regulated (>4-fold); A1S_0095 and A1S_1336, as determined by our microarray data. Comparative qRT-PCR analysis examining the control 17978hm (pWH1266) and complemented 17978hm (pWH0268) strains, using the oligonucleotides listed in Table S1, showed significant up- or down-regulation of the respective genes that were found to be significantly differentially expressed in strain 17978hm as compared to the WT strain by microarray (Table 2). Noteworthy, three of the investigated genes are known to be co-regulated by other proteins; A1S_0111 and A1S_0112 by AbaR and A1S_0095 by Lrp, and therefore it is difficult to assess the magnitude of the effect that H-NS exerts on these genes. Nevertheless, successful complementation of the hyper-motile variants at a phenotypic and transcriptional level was shown, confirming that inactivation of H-NS resulted in various alterations including an increased virulence potential and transcriptional changes observed in the hyper-motile mutants.

SUMMARY

This study describes for the first time the role of H-NS in *A. baumannii*. We employed a broad range of phenotypic and genotypic characterization methods to gain insight into *A. baumannii* virulence mechanisms and the role that H-NS plays in their regulation. Phenotypic characterization showed that hydrophobicity, adherence and motility are likely to be co-regulated in strain ATCC 17978. Furthermore, these features may be associated with virulence based on data from a nematode killing assay and increased binding capacity to the A549 eukaryotic lung cell line. Our analyses also provided evidence that the cellular fatty acid composition is linked to

changes in cell surface hydrophobicity, which subsequently may alter the adherence, motility and virulence characteristics. Although these phenotypes appear to be co-regulated in strain ATCC 17978, it is known that *A. baumannii* strains show major variation in their motility and adherence phenotypes (3, 7). Therefore, the role of H-NS is likely to be distinct in other *A. baumannii* strains, which correlates with the function of H-NS as a regulator of non-conserved genomic regions.

Transcriptomic analysis of 17978hm and its parent strain on semi-solid media identified molecular mechanisms that may be responsible for the phenotypic changes described above. The autotransporter encoded by *ata*, which has been proven to play a role in adherence and virulence (52), was heavily up-regulated. Furthermore, the type VI secretion system and a type I pili were found to be up-regulated and these surface presented protein structures are known to affect adherence and virulence in other Gram-negative pathogens, such as *P. aeruginosa* and *E. coli*. Significantly, up-regulation of genes encoding the fatty acid biosynthetic proteins FabG and FabF may explain the increase of C_{17} fatty acids in the hyper-motile mutant as compared to the WT strain. Although FabG has previously been defined as a nucleoid-associated protein in other bacterial genera (64), the regulatory control of *fabG* and *fabF* in the H-NS deficient strain requires further examination.

Bioinformatic analyses using a number of fully sequenced *A. baumannii* genomes assisted in identification of putative H-NS targets. Various genomic regions that were characterized as horizontally-acquired were transcriptionally repressed by H-NS in the WT strain. Furthermore, examination of the upstream regions of highly expressed genes showed that H-NS is likely to bind AT-rich DNA regions, as observed for H-NS in other bacterial genera. The bioinformatics

approach applied here could also be of use when examining the role of H-NS in *A. baumannii* strains other than ATCC 17978.

In summary, the phenotypic, genomic and transcriptomic analyses carried out using strain ATCC 17978 and its hyper-motile derivatives 17978hm and HNSmut88 revealed a significant role for H-NS in the regulation of the *A. baumannii* persistence and virulence associated genes.

ACKNOWLEDGEMENTS

This work was supported by Project Grant 535053 to MHB and ITP from the National Health and Medical Research Council, Australia. BAE is the recipient of a School of Biological Sciences Endeavour International Postgraduate Research Scholarship and KAH is supported by an APD fellowship from the Australian Research Council (DP110102680).

We would like to thank David Apps and Melissa Gregory for assistance with the fatty acid analyses.

REFERENCES

1. **Bergogne-Berezin E, Towner KJ.** 1996. *Acinetobacter* spp. as nosocomial pathogens: microbiological, clinical, and epidemiological features. Clin Microbiol Rev **9:**148-165.
2. **Gordon NC, Wareham DW.** 2010. Multidrug-resistant *Acinetobacter baumannii*: mechanisms of virulence and resistance. Int J Antimicrob Agents **35:**219-226.
3. **Eijkelkamp BA, Stroeher UH, Hassan KA, Papadimitrious MS, Paulsen IT, Brown MH.** 2011. Adherence and motility characteristics of clinical *Acinetobacter baumannii* isolates. FEMS Microbiol Lett **323:**44-51.
4. **Lee JC, Koerten H, van den Broek P, Beekhuizen H, Wolterbeek R, van den Barselaar M, van der Reijden T, van der Meer J, van de Gevel J, Dijkshoorn L.** 2006. Adherence of *Acinetobacter baumannii* strains to human bronchial epithelial cells. Res Microb **157:**360-366.
5. **de Breij A, Dijkshoorn L, Lagendijk E, van der Meer J, Koster A, Bloemberg G, Wolterbeek R, van den Broek P, Nibbering P.** 2010. Do biofilm formation and interactions with human cells explain the clinical success of *Acinetobacter baumannii*? PLoS One **5:**e10732.
6. **Marti S, Rodriguez-Bano J, Catel-Ferreira M, Jouenne T, Vila J, Seifert H, De E.** 2011. Biofilm formation at the solid-liquid and air-liquid interfaces by *Acinetobacter* species. BMC Res Notes **4:**5.
7. **McQueary CN, Actis LA.** 2011. *Acinetobacter baumannii* biofilms: Variations among strains and correlations with other cell properties. J Microbiol **49:**243-250.

8. **Pour NK, Dusane DH, Dhakephalkar PK, Zamin FR, Zinjarde SS, Chopade BA.** 2011. Biofilm formation by *Acinetobacter baumannii* strains isolated from urinary tract infection and urinary catheters. FEMS Immunol Med Microbiol **62:**328-338.

9. **Rodriguez-Bano J, Marti S, Soto S, Fernandez-Cuenca F, Cisneros JM, Pachon J, Pascual A, Martinez-Martinez L, McQueary C, Actis LA, Vila J.** 2008. Biofilm formation in *Acinetobacter baumannii*: associated features and clinical implications. Clin Microbiol Infect **14:**276-278.

10. **Eijkelkamp BA, Hassan KA, Paulsen IT, Brown MH.** 2011. Investigation of the human pathogen *Acinetobacter baumannii* under iron limiting conditions. BMC Genomics **12:**126.

11. **Mussi MA, Gaddy JA, Cabruja M, Arivett BA, Viale AM, Rasia R, Actis LA.** 2010. The opportunistic human pathogen *Acinetobacter baumannii* senses and responds to light. J. Bacteriol. **192:**6336-6345.

12. **Clemmer KM, Bonomo RA, Rather PN.** 2011. Genetic analysis of surface motility in Acinetobacter baumannii. Microbiology **157:**2534-2544.

13. **Han X, Kennan RM, Davies JK, Reddacliff LA, Dhungyel OP, Whittington RJ, Turnbull L, Whitchurch CB, Rood JI.** 2008. Twitching motility is essential for virulence in *Dichelobacter nodosus*. J. Bacteriol. **190:**3323-3335.

14. **Alarcon I, Evans DJ, Fleiszig SM.** 2009. The role of twitching motility in *Pseudomonas aeruginosa* exit from and translocation of corneal epithelial cells. Invest Ophthalmol Vis Sci **50:**2237-2244.

15. **Stewart RM, Wiehlmann L, Ashelford KE, Preston SJ, Frimmersdorf E, Campbell BJ, Neal TJ, Hall N, Tuft S, Kaye SB, Winstanley C.** 2011. Genetic characterization

indicates that a specific subpopulation of *Pseudomonas aeruginosa* is associated with keratitis infections. J Clin Microbiol **49:**993-1003.

16. **Winstanley C, Kaye SB, Neal TJ, Chilton HJ, Miksch S, Hart CA.** 2005. Genotypic and phenotypic characteristics of *Pseudomonas aeruginosa* isolates associated with ulcerative keratitis. J Med Microbiol **54:**519-526.

17. **Zolfaghar I, Evans DJ, Fleiszig SM.** 2003. Twitching motility contributes to the role of pili in corneal infection caused by *Pseudomonas aeruginosa*. Infect Immun **71:**5389-5393.

18. **Klausen M, Aaes-Jorgensen A, Molin S, Tolker-Nielsen T.** 2003. Involvement of bacterial migration in the development of complex multicellular structures in *Pseudomonas aeruginosa* biofilms. Mol Microbiol **50:**61-68.

19. **Cerqueira GM, Peleg AY.** 2011. Insights into *Acinetobacter baumannii* pathogenicity. IUBMB Life **63:**1055-1060.

20. **Choi CH, Lee JS, Lee YC, Park TI, Lee JC.** 2008. *Acinetobacter baumannii* invades epithelial cells and outer membrane protein A mediates interactions with epithelial cells. BMC Microbiol **8:**216.

21. **Gaddy JA, Tomaras AP, Actis LA.** 2009. The *Acinetobacter baumannii* 19606 OmpA protein plays a role in biofilm formation on abiotic surfaces and in the interaction of this pathogen with eukaryotic cells. Infect Immun **77:**3150-3160.

22. **Choi CH, Lee EY, Lee YC, Park TI, Kim HJ, Hyun SH, Kim SA, Lee SK, Lee JC.** 2005. Outer membrane protein 38 of *Acinetobacter baumannii* localizes to the mitochondria and induces apoptosis of epithelial cells. Cell Microbiol **7:**1127-1138.

572 23. **McConnell MJ, Pachon J.** 2011. Expression, purification, and refolding of biologically
573 active *Acinetobacter baumannii* OmpA from *Escherichia coli* inclusion bodies. Protein
574 Expr Purif **77:**98-103.
575 24. **Ofori-Darko E, Zavros Y, Rieder G, Tarle SA, Van Antwerp M, Merchant JL.** 2000.
576 An OmpA-like protein from *Acinetobacter* spp. stimulates gastrin and interleukin-8
577 promoters. Infect Immun **68:**3657-3666.
578 25. **Luke NR, Sauberan SL, Russo TA, Beanan JM, Olson R, Loehfelm TW, Cox AD, St**
579 **Michael F, Vinogradov EV, Campagnari AA.** 2010. Identification and characterization
580 of a glycosyltransferase involved in *Acinetobacter baumannii* lipopolysaccharide core
581 biosynthesis. Infect Immun **78:**2017-2023.
582 26. **Jacobs AC, Hood I, Boyd KL, Olson PD, Morrison JM, Carson S, Sayood K, Iwen**
583 **PC, Skaar EP, Dunman PM.** 2010. Inactivation of phospholipase D diminishes
584 *Acinetobacter baumannii* pathogenesis. Infect Immun **78:**1952-1962.
585 27. **Russo TA, MacDonald U, Beanan JM, Olson R, MacDonald IJ, Sauberan SL, Luke**
586 **NR, Schultz LW, Umland TC.** 2009. Penicillin-binding protein 7/8 contributes to the
587 survival of *Acinetobacter baumannii in vitro* and *in vivo*. J Infect Dis **199:**513-521.
588 28. **Russo TA, Luke NR, Beanan JM, Olson R, Sauberan SL, MacDonald U, Schultz**
589 **LW, Umland TC, Campagnari AA.** 2010. The K1 capsular polysaccharide of
590 *Acinetobacter baumannii* strain 307-0294 is a major virulence factor. Infect Immun
591 **78:**3993-4000.
592 29. **Gaddy JA, Arivett BA, McConnell MJ, Lopez-Rojas R, Pachon J, Actis LA.** 2012.
593 Role of acinetobactin-mediated iron acquisition functions in the interaction of

Acinetobacter baumannii strain ATCC 19606T with human lung epithelial cells, *Galleria mellonella* caterpillars, and mice. Infect Immun **80:**1015-1024.

30. **Smith MG, Gianoulis TA, Pukatzki S, Mekalanos JJ, Ornston LN, Gerstein M, Snyder M.** 2007. New insights into *Acinetobacter baumannii* pathogenesis revealed by high-density pyrosequencing and transposon mutagenesis. Genes Dev **21:**601-614.

31. **Henry R, Vithanage N, Harrison P, Seemann T, Coutts S, Moffatt JH, Nation RL, Li J, Harper M, Adler B, Boyce JD.** 2012. Colistin-resistant, lipopolysaccharide-deficient *Acinetobacter baumannii* responds to lipopolysaccharide loss through increased expression of genes involved in the synthesis and transport of lipoproteins, phospholipids, and poly-beta-1,6-N-acetylglucosamine. Antimicrob Agents Chemother **56:**59-69.

32. **Daniel C, Haentjens S, Bissinger MC, Courcol RJ.** 1999. Characterization of the *Acinetobacter baumannii* Fur regulator: cloning and sequencing of the *fur* homolog gene. FEMS Microbiol Lett **170:**199-209.

33. **Bhargava N, Sharma P, Capalash N.** 2010. Quorum sensing in *Acinetobacter*: an emerging pathogen. Crit Rev Microbiol **36:**349-360.

34. **Gaddy JA, Actis LA.** 2009. Regulation of *Acinetobacter baumannii* biofilm formation. Future Microbiol **4:**273-278.

35. **Tomaras AP, Flagler MJ, Dorsey CW, Gaddy JA, Actis LA.** 2008. Characterization of a two-component regulatory system from *Acinetobacter baumannii* that controls biofilm formation and cellular morphology. Microbiology **154:**3398-3409.

36. **Rimsky S.** 2004. Structure of the histone-like protein H-NS and its role in regulation and genome superstructure. Curr Opin Microbiol **7:**109-114.

37. **Lang B, Blot N, Bouffartigues E, Buckle M, Geertz M, Gualerzi CO, Mavathur R, Muskhelishvili G, Pon CL, Rimsky S, Stella S, Babu MM, Travers A.** 2007. High-affinity DNA binding sites for H-NS provide a molecular basis for selective silencing within proteobacterial genomes. Nucleic Acids Res **35:**6330-6337.

38. **Brenner S.** 1974. The genetics of *Caenorhabditis elegans*. Genetics **77:**71-94.

39. **Rosenberg M, Gutnick D, Rosenberg E.** 1980. Adherence of bacteria to hydrocarbons: a simple method for measuring cell-surface hydrophobicity. FEMS Microbiol Lett **9:**29-33.

40. **Gregory MK, See VH, Gibson RA, Schuller KA.** 2010. Cloning and functional characterisation of a fatty acyl elongase from southern bluefin tuna (*Thunnus maccoyii*). Comp Biochem Physiol B Biochem Mol Biol **155:**178-185.

41. **Rozen S, Skaletsky H.** 2000. Primer3 on the WWW for general users and for biologist programmers. Methods Mol Biol **132:**365-386.

42. **Livak KJ, Schmittgen TD.** 2001. Analysis of relative gene expression data using real-time quantitative PCR and the 2(-Delta Delta C(T)) Method. Methods **25:**402-408.

43. **Zerbino DR, Birney E.** 2008. Velvet: algorithms for de novo short read assembly using de Bruijn graphs. Genome Res **18:**821-829.

44. **Hunger M, Schmucker R, Kishan V, Hillen W.** 1990. Analysis and nucleotide sequence of an origin of DNA replication in *Acinetobacter calcoaceticus* and its use for *Escherichia coli* shuttle plasmids. Gene **87:**45-51.

45. **Arora K, Whiteford DC, Lau-Bonilla D, Davitt CM, Dahl JL.** 2008. Inactivation of *lsr2* results in a hypermotile phenotype in *Mycobacterium smegmatis*. J. Bacteriol. **190:**4291-4300.

46. **Cordeiro TN, Schmidt H, Madrid C, Juarez A, Bernado P, Griesinger C, Garcia J, Pons M.** 2011. Indirect DNA readout by an H-NS related protein: structure of the DNA complex of the C-terminal domain of Ler. PLoS Pathog **7:**e1002380.

47. **Gordon BR, Li Y, Cote A, Weirauch MT, Ding P, Hughes TR, Navarre WW, Xia B, Liu J.** 2011. Structural basis for recognition of AT-rich DNA by unrelated xenogeneic silencing proteins. P.N.A.S. **108:**10690-10695.

48. **Liang Y, Gao H, Chen J, Dong Y, Wu L, He Z, Liu X, Qiu G, Zhou J.** 2010. Pellicle formation in *Shewanella oneidensis*. BMC Microbiol **10:**291.

49. **de Breij A, Gaddy J, van der Meer J, Koning R, Koster A, van den Broek P, Actis L, Nibbering P, Dijkshoorn L.** 2009. CsuA/BABCDE-dependent pili are not involved in the adherence of *Acinetobacter baumannii* ATCC19606(T) to human airway epithelial cells and their inflammatory response. Res Microb **160:**213-218.

50. **Talbot UM, Paton AW, Paton JC.** 1996. Uptake of *Streptococcus pneumoniae* by respiratory epithelial cells. Infect Immun **64:**3772-3777.

51. **Moorman MA, Thelemann CA, Zhou S, Pestka JJ, Linz JE, Ryser ET.** 2008. Altered hydrophobicity and membrane composition in stress-adapted *Listeria innocua*. J Food Prot **71:**182-185.

52. **Bentancor LV, Camacho-Peiro A, Bozkurt-Guzel C, Pier GB, Maira-Litran T.** 2012. Identification of Ata, a multifunctional trimeric autotransporter of *Acinetobacter baumannii*. J. Bacteriol. **194:**3950-3960.

53. **Mougous JD, Cuff ME, Raunser S, Shen A, Zhou M, Gifford CA, Goodman AL, Joachimiak G, Ordonez CL, Lory S, Walz T, Joachimiak A, Mekalanos JJ.** 2006. A

virulence locus of *Pseudomonas aeruginosa* encodes a protein secretion apparatus. Science **312:**1526-1530.

54. **Weber BS, Miyata ST, Iwashkiw JA, Mortensen BL, Skaar EP, Pukatzki S, Feldman MF.** 2013. Genomic and Functional Analysis of the Type VI Secretion System in *Acinetobacter*. PLoS One **8:**e55142.

55. **Shin JH, Lee HW, Kim SM, Kim J.** 2009. Proteomic analysis of *Acinetobacter baumannii* in biofilm and planktonic growth mode. J Microbiol **47:**728-735.

56. **Zhang YM, Rock CO.** 2008. Membrane lipid homeostasis in bacteria. Nat Rev Microbiol **6:**222-233.

57. **Tremblay J, Deziel E.** 2010. Gene expression in *Pseudomonas aeruginosa* swarming motility. BMC Genomics **11:**587.

58. **Kahramanoglou C, Seshasayee AS, Prieto AI, Ibberson D, Schmidt S, Zimmermann J, Benes V, Fraser GM, Luscombe NM.** 2011. Direct and indirect effects of H-NS and Fis on global gene expression control in *Escherichia coli*. Nucleic Acids Res **39:**2073-2091.

59. **Dorman CJ, Kane KA.** 2009. DNA bridging and antibridging: a role for bacterial nucleoid-associated proteins in regulating the expression of laterally acquired genes. FEMS Microbiol Rev **33:**587-592.

60. **Bernard CS, Brunet YR, Gueguen E, Cascales E.** 2010. Nooks and crannies in type VI secretion regulation. J. Bacteriol. **192:**3850-3860.

61. **Darling AC, Mau B, Blattner FR, Perna NT.** 2004. Mauve: multiple alignment of conserved genomic sequence with rearrangements. Genome Res **14:**1394-1403.

62. **Allsopp LP, Beloin C, Ulett GC, Valle J, Totsika M, Sherlock O, Ghigo JM, Schembri MA.** 2012. Molecular characterization of UpaB and UpaC, two new autotransporter proteins of uropathogenic *Escherichia coli* CFT073. Infect Immun **80:**321-332.

63. **Sun W, Xu X, Pavlova M, Edwards AM, Joachimiak A, Savchenko A, Christendat D.** 2005. The crystal structure of a novel SAM-dependent methyltransferase PH1915 from *Pyrococcus horikoshii*. Protein Sci **14:**3121-3128.

64. **Ohniwa RL, Ushijima Y, Saito S, Morikawa K.** 2011. Proteomic analyses of nucleoid-associated proteins in *Escherichia coli*, *Pseudomonas aeruginosa*, *Bacillus subtilis*, and *Staphylococcus aureus*. PLoS One **6:**e19172.

FIGURE LEGENDS

Fig 1

Genetic characteristics of the hyper-motile *A. baumannii* strains. (A) Using whole genome sequencing of the ATCC 17978 and 17978hm strains, an insertion sequence (IS) element was identified in a position unique to *A. baumannii* strain 17978hm. The sequence as found in strain 17978hm has been provided; the target sites of the IS element are shown in red and the inverted repeat section of the IS element underlined. (B) Amino acid sequences of the DNA binding region of the H-NS-like proteins from strain ATCC 17978, HNSmut88, *Mycobacterium tuberculosis*, *Salmonella* and *E. coli* are displayed. Positively charged residues that may be involved in DNA interactions are shown in red. The arginine (R) residues positioned outside of the DNA binding domain are in bold. The lysine (K) in position 88 in strain ATCC 17978 mutated to an isoleucine (I) in strain HNSmut88 is boxed in blue.

Fig 2

Adherence characteristics of strains ATCC 17978 and 17978hm. (A) Pellicles of *A. baumannii* strains ATCC 17978 and 17978hm were examined after incubation for 72 hours at 25°C and statistically significant ($p<0.001$; two-tailed Student's *t*-test) differences are indicated by asterisks. Experiments were performed at least three times, error bars represent the standard deviation. (B) The number of colony forming units (CFUs) in Log_{10} values of *A. baumannii* ATCC 17978, 17978hm, 17978hm (pWH1266) and 17978hm (pWH0268) recovered from a washed A549 cell culture after incubation for 4 hours were enumerated. Significant differences between ATCC 17978 and 17978hm ($p<0.05$), and 17978hm (pWH1266) and 17978hm

716 (pWH0268) ($p<0.005$) were observed using a two-tailed Student's *t*-test and are indicated by
717 asterisks. Error bars show the standard error of the mean.

718 Fig 3

719 Examination of the virulence potential of ATCC 17978 and 17978hm. The virulence potential of
720 *A. baumannii* strains ATCC 17978 and 17978hm was examined by counting live versus dead *C.*
721 *elegans* nematodes grown on a lawn of the respective *A. baumannii* test strains. Significant
722 differences ($p<0.001$) in killing were observed at 120 hours and 144 hours as determined by
723 student's *t*-test and are indicated by asterisks. The error bars show the standard deviation (n=4).

724 Fig 4

725 Overview of the transcriptional differences between motile and non-motile *A. baumannii* cells.
726 Comparative transcriptomics are displayed as the differential expression (in Log_2-values) of
727 strains 17978hm (motile) and ATCC 17978 (non-motile) harvested from semi-solid MH media
728 (0.25% agar). Diamond markers indicate the differential expression levels of all predicted open
729 reading frames of the ATCC 17978 genome and are sorted on the X-axis according to the locus-
730 tag. The dashed lines indicate 4-fold ($Log_2=2$) differential expression; up-regulated genes in
731 motile populations are located above the green line and down-regulated genes below the red line.
732 Examples of differentially expressed genes have been indicated in the figure, such as the genes
733 involved in biosynthesis of quorum-sensing signals and those encoding proteins of the
734 phenylacetic acid degradation pathway.

735 Fig 5

736 Bioinformatic analysis of the putative H-NS targets in the ATCC 17978 genome. Transcriptome
737 results were mapped onto a circular representation of *A. baumannii* ATCC 17978 (CP000521)
738 using CGview. Up-regulated genes are represented in green and down-regulated genes in red;
739 half-sized bars equal 2-4-fold differential expression and full-sized bars >4-fold. To identify
740 potentially horizontally-acquired genomic regions, comparative Blastp analyses between
741 CP000521 (outer ring) and *A. baumannii* AB0057 (brown), ACICU (blue), AYE (purple),
742 AB307-0294 (orange), SDF (turquoise) and *A. baylyi* ADP1 (grey) are included. Various up-
743 regulated genes or gene clusters not fully conserved between CP000521 and other genomes were
744 identified; these were subsequently examined using Mauve. Based on CGview and Mauve
745 analyses, the following 13 up-regulated genes or gene clusters were found to be horizontally-
746 acquired and therefore putative H-NS target sites: (1) A1S_0519-0525 fatty acid biosynthesis;
747 (2) A1S_0745 bacterial surface protein; (3) A1S_1032-1033 Ata and a putative antigen; (4)
748 A1S_1078-1079 hypothetical protein and dichlorophenol hydroxylase; (5) A1S_1357 alanine
749 racemase; (6) A1S_2271 RNA splicing ligase; (7) A1S_2396 transcriptional regulator; (8)
750 A1S_2509 putative chaperone; (9) A1S_2648-2649 putative regulatory proteins; (10) A1S_2744
751 S-adenosyl-L-methionine-dependent methyltransferase; (11) A1S_2789 metallopeptidase; (12)
752 A1S_3273 putative secreted protein; and (13) A1S_3397 lysine (LysE) or homoserine/threonine
753 resistance (RhtB) protein.

754 Fig 6

755 GC-percentage of the putative H-NS targets. The GC-content plots are shown above schematic
756 representations of genes differentially expressed in the *hns* mutant strain, 17978hm, with their

757 respective locus-tag number displayed underneath. The average GC-percentage has been
758 calculated over the regions located upstream of these highly up-regulated genes and is
759 highlighted in blue. The GC-content plots were derived from the *A. baumannii* ATCC 17978
760 (CP000521) genome displayed in UGENE v1.10.1 (UniPro). These regions have a GC-
761 percentage significantly lower than the average genome-wide intergenic regions (~35%) and may
762 form suitable H-NS binding sites.

Table 1

Cell surface hydrophobicity and fatty acid composition.

Strains	Hydrophobicity index (StDev)	Fatty acid percentage		
		15:0	16:0	17:0
ATCC 17978	44 (13.1)	1.9	29.1	3.4
17978hm	65 (6.4)	2.8	25.4	6.9
17978hm (pWH1266)	64 (3.3)	2.4	24.4	5.2
17978hm (pWH0268)	14 (0.1)	0.7	31.4	2.6

Supplementary Table 1

Oligonucleotides used in this study.

Name/target	Forward 5' -> 3'	Reverse 5' -> 3'
A1S_r01 (*16S rRNA*)[a]	CAGCTCGTGTCGTGAGATGT	CGTAAGGGCCATGATGACTT
A1S_0111	TTGGTCGAGTCAATCTGCAA	CTCGGGTCCCAATAAAATCA
A1S_0112	ACGCCAGTCTGGTGGTATTC	AGGTTCGAACAGCAATACGG
A1S_1032	AAGCCAGTCAAGCAACTGGT	TCAGAATCTGCTGCACCATC
A1S_1292	ACGCAACGCGTAATAAAGTG	TAAAGGGTCAAAAGGCGAAC
A1S_1509	CCAAGGAAGGCGCTGT	TTGGGGAATGGCTTGC
A1S_1699	CAAAGACATTGCTGGTCGTG	AATCACGCTTGGACCTTCAC
A1S_3273	GGGTACACCTTCAGCAGAGC	GCACCATATTTACGGGCAAC
A1S_0095	CCGCAAAGTTATGCTGTGAA	GACGTAAACCCGTCCAGAAA
A1S_1336	CGTGCGATGGTACGTATTTG	ACGGTTCACTGCATCTTGTG
A1S_0268	GAGAGGATCCATAAATATTA AGAAAATATATTAC	GAGAGGATCCTTAGATTAAGAA ATCTTCAAG
A1S_2562	CACCATGAATATGCTCAAAGA CAT	GGTTGAAATGGTCTCACCAACTG G

[a] Oligonucleotide sequences obtained from **Higgins *et al.*** 2004 J Antimicrob Chemother **54**: 821-823.

Supplementary Table 2

Genes up-regulated more than 4-fold in strain 17978hm

Locus-tag	Gene product	Times-fold difference
A1S_0109	homoserine lactone synthase	30.7
A1S_0110	hypothetical protein	7.9
A1S_0111	eR transcriptional regulator	5.7
A1S_0112	Acyl-CoA synthetase/AMP-acid ligases II	558.6
A1S_0113	Acyl-CoA dehydrogenase	536.6
A1S_0114	Acyl carrier protein	727.2
A1S_0115	Amino acid adenylation	611.4
A1S_0116	RND superfamily-like exporters	240.6
A1S_0117	hypothetical protein	211.4
A1S_0118	hypothetical protein	53.8
A1S_0119	Phosphopantethiene-protein transferase	47.1
A1S_0628	putative transposase	42.9
A1S_0739	putative transcriptional regulator	4.1
A1S_0745	hypothetical protein	21.7
A1S_0921	arginine/ornithine antiporter	4.5
A1S_0922	putative homocysteine S-methyltransferase family protein	4.3
A1S_1032	hypothetical protein	10.0
A1S_1033	putative antigen	8.0
A1S_1078	hypothetical protein	6.4
A1S_1079	dichlorophenol hydroxylase (EC:1.14.13.20)	10.6
A1S_1081	putative transcriptional regulator	6.2
A1S_1256	putative transcriptional regulator	21.4
A1S_1272	putative transcriptional regulator	4.8
A1S_1292	putative signal peptide	49.0
A1S_1293	hypothetical protein	35.7
A1S_1294	hypothetical protein	34.4
A1S_1295	hypothetical protein	13.5
A1S_1296	hypothetical protein	4.6
A1S_1297	hypothetical protein	5.8
A1S_1304	hypothetical protein	4.7
A1S_1357	alanine racemase	70.9
A1S_1384	CinA-like protein	5.7
A1S_1404	putative cysteine desulfurase 1 (Csd)	4.7
A1S_1405	putative cysteine desulfurase 1 (Csd)	5.7
A1S_1406	major membrane protein I (MMP-I)	5.8
A1S_1407	serine acetyltransferase	4.4
A1S_1408	putative rhodanese-related sulfurtransferase	5.2
A1S_1438	putative coenzyme F420-dependent N5N10-methylene tetrahydromethanopterin reductase	12.9
A1S_1439	putative coenzyme F420-dependent N5N10-methylene tetrahydromethanopterin reductase	16.8
A1S_1440	putative transporter (MFS superfamily)	4.2
A1S_1507	fimbrial protein	13.8
A1S_1508	fimbrial biogenesis outer membrane usher protein	18.3
A1S_1509	pili assembly chaperone	17.2
A1S_1510	fimbrial protein	12.2
A1S_1699	acetoin:26-dichlorophenolindophenol oxidoreductase alpha subunit	7.4
A1S_1700	acetoin:26-dichlorophenolindophenol oxidoreductase beta subunit (EC:1.2.4.1)	7.3
A1S_1701	dihydrolipoamide acetyltransferase	5.5
A1S_1702	dihydrolipoamide dehydrogenase	6.2
A1S_1703	dihydrolipoamide dehydrogenase	6.7
A1S_1751	AdeA membrane fusion protein	8.7
A1S_1769	putative RND family drug transporter	5.1
A1S_1770	hypothetical protein	5.3
A1S_2396	putative transcriptional regulator	4.1
A1S_2554	putative transposase	27.6
A1S_2647	putative transcriptional regulator	4.1
A1S_2648	hypothetical protein	6.9
A1S_2649	putative regulatory protein	6.9
A1S_3104	putative ATP-dependent RNA helicase	4.5
A1S_3120	hypothetical protein	4.2
A1S_3146	multidrug efflux transport protein	4.1
A1S_3273	putative peptide signal	4.8

Genes down-regulated more than 4-fold in strain 17978hm

Locus-tag	Gene product	Times-fold difference
A1S_1186	ATP-dependent protease Hsp 100	-26.7
A1S_2183	putative signal peptide	-21.1
A1S_1950	putative universal stress protein	-19.9
A1S_0095	D-amino acid dehydrogenase (EC:1.4.99.1)	-17.4
A1S_0771	hypothetical protein	-16.6
A1S_3113	hypothetical protein	-16.0
A1S_3350	hypothetical protein	-14.4
A1S_2195	hypothetical protein	-12.6
A1S_1708	beta-lactamase-like protein	-12.2
A1S_3317	putative outer membrane protein	-12.2
A1S_1030	DNA-binding ATP-dependent protease La	-12.1
A1S_1932	hypothetical protein	-10.9
A1S_2960	chaperone Hsp70	-10.6
A1S_0096	alanine racemase 2 PLP-binding, catabolic	-9.7
A1S_2093	hypothetical protein	-8.9
A1S_0558	aconitate hydratase 1 (EC:4.2.1.3)	-8.8
A1S_1193	OmpA/MotB	-8.8
A1S_3175	bacterioferritin	-8.6
A1S_2070	P-type ATPase Mg2+ ATPase transporter (EC:3.6.3.2)	-8.4
A1S_1031	DNA-binding ATP-dependent protease La	-8.2
A1S_1687	transcriptional regulator	-8.1
A1S_1338	hypothetical protein	-8.1
A1S_0800	bacterioferritin	-8.0
A1S_1046	Lysine exporter protein (LysE/YggA)	-7.9
A1S_3023	hypothetical protein	-7.8
A1S_1984	D-amino acid dehydrogenase small subunit	-7.7
A1S_0363	hypothetical protein	-7.2
A1S_0683	putative sigma (54) modulation protein RpoX	-6.9
A1S_2538	outer membrane protein CarO precursor	-6.8
A1S_1266	hypothetical protein	-6.8
A1S_1337	Phenylacetic acid degradation B	-6.7
A1S_2820	hypothetical protein	-6.7
A1S_1339	Phenylacetate-CoA oxygenase PaaJ subunit	-6.6
A1S_3277	putative pirin-like protein	-6.5
A1S_0301	hypothetical protein	-6.5
A1S_1267	putative lactam utilization protein	-6.4
A1S_1910	ATP-binding protease component	-6.4
A1S_1246	putative universal stress protein	-6.1
A1S_0445	hypothetical protein	-6.1
A1S_0097	hypothetical protein	-6.1
A1S_1270	hypothetical protein	-5.9
A1S_3046	oligopeptidase A	-5.8
A1S_2296	putative protease	-5.8
A1S_1269	putative allophanate hydrolase subunit 1 and 2	-5.8
A1S_1340	Phenylacetate-CoA oxygenase/reductase PaaK subunit	-5.8
A1S_2809	bacteriolytic lipoprotein entericidin B	-5.8
A1S_1343	PaaC	-5.7
A1S_1268	hypothetical protein	-5.6
A1S_2616	hypothetical protein	-5.5
A1S_0210	transposase	-5.5
A1S_2664	chaperone Hsp60	-5.4
A1S_2291	hypothetical protein	-5.3
A1S_1342	putative enoyl-CoA hydratase II	-5.3
A1S_2450	putative pyruvate decarboxylase	-5.2
A1S_2259	putative signal peptide	-5.2
A1S_2840	outer membrane protein A	-5.2
A1S_2959	Hsp 24 nucleotide exchange factor	-5.1
A1S_1925	cytochrome d terminal oxidase polypeptide subunit II	-5.1
A1S_1433	ubiquinol oxidase subunit II	-5.1
A1S_0207	hypothetical protein	-5.1
A1S_0646	lcmB protein	-5.0
A1S_2449	aromatic amino acid transporter (APC family)	-5.0
A1S_0172	hypothetical protein	-5.0
A1S_2072	putative universal stress protein family	-4.9
A1S_1518	putative suppressor of F exclusion of phage T7	-4.9
A1S_1390	hypothetical protein	-4.8
A1S_1862	hypothetical protein	-4.8
A1S_0496	putative phosphatidylglycerophosphatase B	-4.7
A1S_0412	catalase (EC:1.11.1.6)	-4.7
A1S_1926	hypothetical protein	-4.7
A1S_0884	putative outer membrane protein	-4.7
A1S_1726	aspartate ammonia-lyase (aspartase) (EC:4.3.1.1)	-4.6
A1S_2416	hypothetical protein	-4.6
A1S_3180	putative signal peptide	-4.5
A1S_1335	Phenylacetic acid degradation protein paaN	-4.5
A1S_1924	cytochrome d terminal oxidase polypeptide subunit I	-4.4
A1S_1861	benzoate dioxygenase large subunit	-4.4
A1S_0627	hypothetical protein	-4.4
A1S_2417	starvation-induced peptide utilization protein	-4.3
A1S_0642	hypothetical protein	-4.3
A1S_1336	hypothetical protein	-4.2
A1S_1859	aromatic-ring-hydroxylating dioxygenase beta subunit	-4.2
A1S_2696	hypothetical protein	-4.2
A1S_3122	hypothetical protein	-4.2
A1S_2092	aminopeptidase N	-4.1
A1S_0299	hypothetical protein	-4.1
A1S_2886	acyl-CoA dehydrogenase	-4.1
A1S_0465	Sec-independent protein translocase protein	-4.1
A1S_0634	hypothetical protein	-4.0
A1S_3246	hypothetical protein	-4.0
A1S_2504	excinuclease ABC subunit B	-4.0

Supplementary Table 3

PM1 MicroPlate™CarbonSources

A1 Negative Control	A2 L-Arabinose	A3 N-Acetyl-D-Glucosamine	A4 D-Saccharic Acid	A5 Succinic Acid	A6 D-Galactose	A7 L-Aspartic Acid	A8 L-Proline	A9 D-Alanine	A10 D-Trehalose	A11 D-Mannose	A12 Dulcitol
B1 D-Serine	B2 D-Sorbitol	B3 Glycerol	B4 L-Fucose	B5 D-Glucuronic Acid	B6 D-Gluconic Acid	B7 D,L-α-Glycerol-Phosphate	B8 D-Xylose	B9 L-Lactic Acid	B10 Formic Acid	B11 D-Mannitol	B12 L-Glutamic Acid
C1 D-Glucose-6-Phosphate	C2 D-Galactonic Acid-γ-lactone	C3 D,L-Malic Acid	C4 D-Ribose	C5 Tween 20	C6 L-Rhamnose	C7 D-Fructose	C8 Acetic Acid	C9 α-D-Glucose	C10 Maltose	C11 D-Melibiose	C12 Thymidine
D1 L-Asparagine	D2 D-Aspartic Acid	D3 D-Glucosaminic Acid	D4 1,2-Propanediol	D5 Tween 40	D6 α-Keto-Glutaric Acid	D7 α-Keto-Butyric Acid	D8 α-Methyl-D-Galactoside	D9 α-D-Lactose	D10 Lactulose	D11 Sucrose	D12 Uridine
E1 L-Glutamine	E2 M-Tartaric Acid	E3 D-Glucose-1-Phosphate	E4 D-Fructose-6-Phosphate	E5 Tween 80	E6 α-Hydroxy Glutaric Acid -γ-Lactone	E7 α-Hydroxy Butyric Acid	E8 ß-Methyl-D-Glucoside	E9 Adonitol	E10 Maltotriose	E11 2-Deoxy Adenosine	E12 Adenosine
F1 Glycyl-L-Aspartic Acid	F2 Citric Acid	F3 M-Inositol	F4 D-Threonine	F5 Fumaric Acid	F6 Bromo Succinic Acid	F7 Propionic Acid	F8 Mucic Acid	F9 Glycolic Acid	F10 Glyoxylic Acid	F11 D-Cellobiose	F12 Inosine
G1 Glycyl-L-Glutamic Acid	G2 Tricarballylic Acid	G3 L-Serine	G4 L-Threonine	G5 L-Alanine	G6 L-Alanyl-Glycine	G7 Acetoacetic Acid	G8 N-Acetyl-ß -D-Mannosamine	G9 Mono Methyl Succinate	G10 Methyl Pyruvate	G11 D-Malic Acid	G12 L-Malic Acid
H1 Glycyl-L-Proline	H2 p-Hydroxy Phenyl Acetic Acid	H3 m-Hydroxy Phenyl Acetic Acid	H4 Tyramine	H5 D-Psicose	H6 L-Lyxose	H7 Glucuronamide	H8 Pyruvic Acid	H9 L-Galactonic Acid-Lactone	H10 D-Galacturonic Acid	H11 Phenylethylamine	H12 2-Aminoethanol

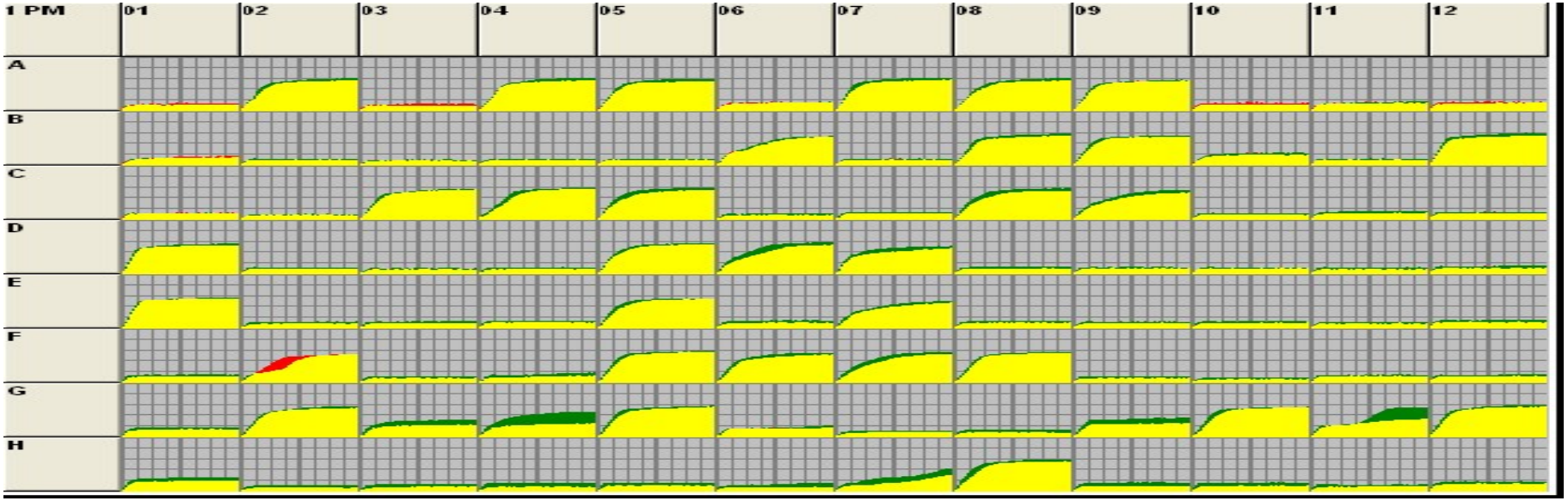

PM2A MicroPlate™CarbonSources
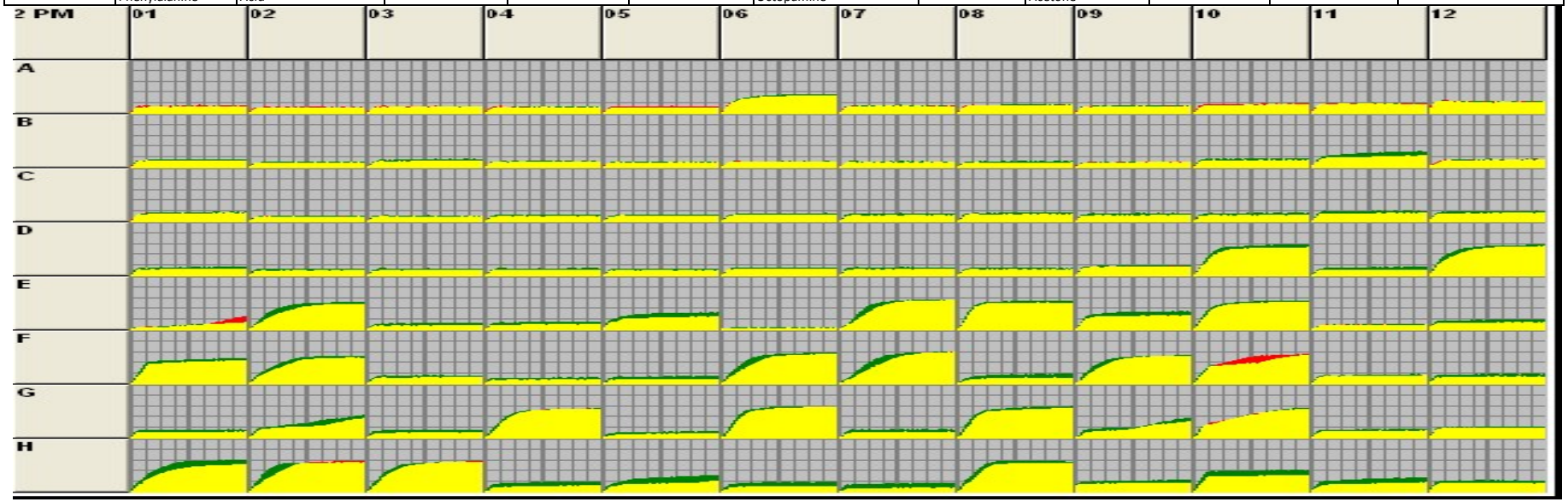
A1 Negative Control	A2 Chondroitin Sulfate C	A3 α-Cyclodextrin	A4 ß-Cyclodextrin	A5 γ-Cyclodextrin	A6 Dextrin	A7 Gelatin	A8 Glycogen	A9 Inulin	A10 Laminarin	A11 Mannan	A12 Pectin
B1 N-Acetyl-D- Galactosamine	B2 N-Acetyl- Neuraminic Acid	B3 ß-D-Allose	B4 Amygdalin	B5 D-Arabinose	B6 D-Arabitol	B7 L-Arabitol	B8 Arbutin	B9 2-Deoxy-D- Ribose	B10 I-Erythritol	B11 D-Fucose	B12 3-0-ß D-Galactopyranosyl D-Arabinose
C1 Gentiobiose	C2 L-Glucose	C3 Lactitol	C4 D-Melezitose	C5 Maltitol	C6 α-Methyl-D- Glucoside	C7 ß-Methyl-D- Galactoside	C8 3-Methyl Glucose	C9 ß-Methyl-D- Glucuronic Acid	C10 α-Methyl-D- Mannoside	C11 ß-Methyl-D- Xyloside	C12 Palatinose
D1 D-Raffinose	D2 Salicin	D3 Sedoheptulosa	D4 L-Sorbose	D5 Stachyose	D6 D-Tagatose	D7 Turanose	D8 Xylitol	D9 N-Acetyl-D- Glucosaminitol	D10 γ-Amino Butyric Acid	D11 d-Amino Valeric Acid	D12 Butyric Acid
E1 Capric Acid	E2 Caproic Acid	E3 Citraconic Acid	E4 Citramalic Acid	E5 D-Glucosamine	E6 2-Hydroxy Benzoic Acid	E7 4-Hydroxy Benzoic Acid	E8 ß-Hydroxy Butyric Acid	E9 γ-Hydroxy Butyric Acid	E10 α-Keto Valeric Acid	E11 Itaconic Acid	E12 5-Keto-D- Gluconic Acid
F1 D-Lactic Acid Methyl Ester	F2 Malonic Acid	F3 Melibionic Acid	F4 Oxalic Acid	F5 Oxalomalic Acid	F6 Quinic Acid	F7 D-Ribono- 1,4-Lactone	F8 Sebacic Acid	F9 Sorbic Acid	F10 Succinamic Acid	F11 D-Tartaric Acid	F12 L-Tartaric Acid
G1 Acetamide	G2 L-Alaninamide	G3 N-Acetyl-L- Glutamic Acid	G4 L-Arginine	G5 Glycine	G6 L-Histidine	G7 L-Homoserine	G8 Hydroxy-L- Proline	G9 L-Isoleucine	G10 L-Leucine	G11 L-Lysine	G12 L-Methionine
H1 L-Ornithine	H2 L- Phenylalanine	H3 L-Pyroglutamic Acid	H4 L-Valine	H5 D,L-Carnitine	H6 Sec-Butylamine	H7 D,L- Octopamine	H8 Putrescine	H9 Dihydroxy Acetone	H10 2,3-Butanediol	H11 2,3-Butanone	H12 3-Hydroxy 2-Butanone